FIRST OCCURRENCE OF A STACKING SEQUENCE INCLUDING (±60°, 180°) ROTATIONS IN Mg-RICH ANNITE

Toshihiro Kogure and Massimo Nespolo[†]

Mineralogical Institute, Graduate School of Science, The University of Tokyo, 7-3-1 Hongo, Bunkyo-Ku, Tokyo 113-0033, Japan

Abstract—Transmission electron microscopy (TEM) observation shows narrow regions in a Ti-containing Mg-rich annite of composition $(K_{0.90}Na_{0.02})(Mg_{0.72}Fe^{2+}_{1.78}Mn_{0.03}Ti_{0.27}Al_{0.05})(Si_{2.77}Al_{1.23})O_{10}(OH,F)_2$ from a granitic rock, where the ±60° and 180° stacking angles occur extensively. These regions are a few hundreds of nanometers thick along the [001]* direction and are within $1M$ or $2M_1$ annite. The stacking sequence in one of these regions was determined by two atomic-resolution images recorded along $[\bar{1}10]$ and [010] of the same crystal. Stacking sequences with ±120° or 180° rotations are dominant, although those with ±60° rotations occur also. Locally $2O$ and more complex sequences exist. Compositional analysis by TEM indicated no difference in the chemical compositions between these regions and the adjacent ones with regular $1M$ or $2M_1$ stacking sequence. The origin of these unusual stacking sequences in annite is discussed.

Key Words—Annite, Biotite, HRTEM, Mica, Polytype-$2O$, Polytypism, Stacking Disorder.

INTRODUCTION

Since the pioneer study of Mauguin (1928), polytypism of micas was extensively investigated, both experimentally and theoretically (see references in Bailey, 1980; Nespolo *et al.*, 1997, 1998). Polytypism in micas occurs owing to six directions of stagger, with a length of $a/3$ in (001) projection, between two tetrahedral sheets in a 2:1 layer. Stacking of these 2:1 layers occurs with respect to the stagger direction (Smith and Yoder, 1956). Polytypes where the position of one layer relative to the other layers is the same or equivalent for all layers are called *homogenous polytypes* (Zvyagin, 1988). Homogeneous polytypes are also known as "simple" (Smith and Yoder, 1956) or "standard" (Bailey, 1980) and are subdivided into three families of MDO (maximum degree of order) polytypes (Backhaus and Ďurovič, 1984). Remaining polytypes are called *inhomogeneous polytypes* (Zvyagin, 1988). Inhomogeneous polytypes are also known as "complex" (Smith and Yoder, 1956). Inhomogeneous polytypes are rare and their occurrence seems to relate to several factors, among which crystal chemistry and crystal-growth conditions are important (Baronnet, 1980).

Classification of mica polytypes may be based on: *subfamily A* [polytypes where (0°, ±120°) rotations occur], *subfamily B* [polytypes where the rotation is (±60°, 180°)], and *mixed-rotation* (polytypes where both types of rotations occur) (Backhaus and Ďurovič, 1984; Nespolo, 1999). These three subfamilies can be distinguished from reflections with $h \neq 0$ (mod 3) and $k = 0$ (mod 3) (orthohexagonal indexing). These are

family reflections (*i.e.*, reflections common to all polytypes based on the same structural principle; Ďurovič and Weiss, 1986) for both subfamilies A and B, but these reflections are "non-family" reflections (characteristic of each polytype) for mixed-rotation polytypes. Along these reciprocal lattice rows, subfamily A, subfamily B, and mixed-rotation polytypes show one, two, and N reflections respectively in the 1 nm^{-1} repeat, where N is the number of layers of the polytype (Nespolo, 1999). Disorder in stacking sequence appears as streaks along reciprocal lattice rows parallel to [001]*. For disorder involving $(2n + 1)60°$ rotations, the streaks are visible along reciprocal lattice rows with $h \neq 0$ (mod 3) and $k = 0$ (mod 3) (Ďurovič *et al.*, 1984; Weiss and Wiewióra, 1986; Bailey, 1988).

Previous work showed that subfamily-A polytypes are more abundant than others, both in natural and synthetic samples. Within subfamily A, the three homogeneous polytypes, identified by Ramsdell (1947) notation as $1M$, $2M_1$, and $3T$, and several inhomogeneous polytypes with more complex stacking sequences have been found (Ross *et al.*, 1966; Nespolo and Takeda, 1999). The latter include $1M_r$-$n(120)$ disordered structures (Ross *et al.*, 1966). Only homogeneous polytypes have been reported in subfamily B. $2M_2$ is relatively common in lithium micas and has been found also in some dioctahedral micas containing high-Al (Drits *et al.*, 1966; Zhukhlistov *et al.*, 1973) or Cs (Ni and Hughes, 1996). $2O$ was found in the brittle mica anandite (Giuseppetti and Tadini, 1972; Filut *et al.*, 1985), but $6H$ is still unknown. The 180° rotation is the least common in micas, where it is known only in anandite-$2O$ (Giuseppetti and Tadini, 1972; Filut *et al.*, 1985) and in fluoropolylithionite-$4A_5$ (Takeda, 1967). The occurrence of $(2n + 1)60°$

[†] Present address: National Institute for Research in Inorganic Materials. 1-1 Namiki, Tsukuba-shi, Ibaraki 305-0044 Japan.

784

rotations in disordered structures of mica-related phyllosilicates was investigated in detail by Drits *et al.* (1984) and Drits and McCarty (1996).

Two reasons may explain why subfamily B and mixed-rotation polytypes occur more rarely than subfamily-A polytypes. 1) A (±60°, 180°) rotation of successive layers produces an unfavorable arrangement of oxygen atoms at the interlayer (Radoslovich, 1959). Because of the rotation of the tetrahedra around [001]* to form a ditrigonal topology (Belov, 1949; Takéuchi and Sadanaga, 1959), basal-oxygen atoms coordinate to the interlayer cation in a trigonal prismatic configuration. This arrangement does not occur in subfamily-A polytypes, where the coordination polyhedron of the interlayer cation is a trigonal antiprism. The occurrence of the $2M_2$ polytype in lithium micas is attributed to the small ditrigonal rotation (Takeda and Burnham, 1969). In addition, fluorine substitutes for OH in association with Li sites (Rieder *et al.,* 1970). Coupled substitutions Al-Al-□-OH → Al-Li-Li-F (where □ represents a vacancy) cause deformation in the octahedral sheet to make the $2M_2$ polytype more favored over $2M_1$ (Takeda *et al.,* 1971). 2) Twinning normal to (001) (Belov, 1949), spiral growth (Baronnet, 1980), lateral impingement (Baronnet, 1973), or lateral coalescence (Sunagawa *et al.,* 1975) are processes which allow two crystals or two portions of a crystal on a plane normal to (001) to come into contact. A coherent interface can form when the two crystals are rotated with respect to each other by (0°, ±120°) and this produces continuity of the octahedral sheet. In contrast, two crystals that are related by a (180°, ±60°) rotation normal to (001) would require a distorted coordination at the interface between the two crystals at the octahedral-sheet junction (Belov, 1949; Baronnet and Amouric, 1986).

X-ray diffraction (XRD) is the common technique to investigate mica polytypes and related phyllosilicates. XRD applications for the study of stacking faults in disordered structures are given in Drits and Tchoubar (1990) and Reynolds (1993). Oblique-texture electron diffraction is also extensively and successfully employed (Zvyagin, 1967; Zvyagin *et al.,* 1979). Iijima and Buseck (1978) showed that stacking sequences in mica polytypes can be determined by observing the stagger direction in each 2:1 layer by using high-resolution transmission electron microscopy (HRTEM). However, as noted by Iijima and Buseck (1978), the application of this technique to investigate mica polytypes (*e.g.,* Tomura *et al.,* 1978; Amouric and Baronnet, 1983; Baronnet and Kang, 1989) was normally not sufficient to determine stacking sequences where (±60°, 180°) rotations occur, because observation was generally done only along [100], [110], or [$\bar{1}$10]. The image from these directions can distinguish the stagger direction of each layer with an angle of (0°, 180°), (60°, 120°), or (−60°, −120°), but not be-

tween the directions within each pair. A second HRTEM image is needed with the specimen rotated by 60° (along corresponding directions of [100], [110], or [$\bar{1}$10]) or 30° (along [310], [010], or [3$\bar{1}$0]). The rotation of the specimen by 60° in a TEM with a high-resolution pole-piece is difficult. On the other hand, analyses of stacking sequences based on images observed along [310], [010], or [3$\bar{1}$0] have not been performed because they require higher resolution images than those observed down [100], [110], or [$\bar{1}$10]. However, the determination of the stacking sequences in mica and chlorite was successful recently by using images from these directions (Banfield and Murakami, 1998; Kogure and Banfield, 1998; Kogure and Nespolo, 1999).

During TEM observation for a study involving alteration of biotite with a Mg-rich annite composition, we found images showing mixed-rotation stacking sequence never reported previously for biotite. The presence of both even and odd rotations is unambiguously confirmed by using the reflections with $h \neq 0$ (mod 3) and $k = 0$ (mod 3) in electron-diffraction patterns.

MATERIAL AND METHODS

The specimen investigated consists of biotite crystals from granite (tonalite) from Gogoshima, Ehime prefecture, Japan (Ochi, 1982). The crystals ranges in size from 0.5 to 2 mm. The average chemical composition of several biotite crystals, determined by electron microprobe analyses, is $(K_{0.90}Na_{0.02})(Mg_{0.72}Fe^{2+}_{1.78}Mn_{0.03}Ti_{0.27}Al_{0.05})(Si_{2.77}Al_{1.23})O_{10}(OH,F)_2$, assuming all iron is ferrous. According to the IMA Committee on Mica Nomenclature (Rieder *et al.,* 1998) the present specimen belongs to the biotite series and should be called "Ti-containing Mg-rich annite". The preparation method of the specimen for TEM observations was described by Ferrow and Roots (1989) and Kogure and Murakami (1996).

TEM analysis was performed at 200 kV using a JEOL JEM-2010 microscope (Cs = 0.5 mm and the corresponding point resolution of 0.20 nm) and using a double-tilt specimen holder, which can tilt the specimen by ±20° about two orthogonal axes. Although this tilt angle is insufficient, a crystal fortuitously oriented can be observed down two zone axes 30° apart as described above. Atomic-resolution images were obtained from thin areas and near Scherzer defocus. Chemical compositions were determined locally by an energy-dispersive X-ray (EDX) detector mounted on the TEM with a take-off angle of 17.5° and a Kevex Sigma spectrum analyzer. The recorded images on films were digitized using a charge-coupled device (CCD) camera. Some digitized images were processed using Gatan Digital Micrograph version 2.5 software. Noise was removed by masking the reciprocal spaces, except for reciprocal-lattice rows along [001]* in the Fourier transform of the images. Image simulations
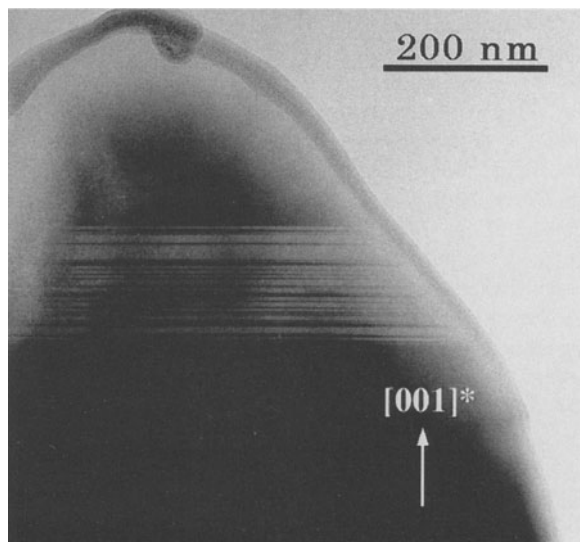
Figure 1. A bright-field image showing band-like contrast in Mg-rich annite. The beam direction is close to, but slightly away from [010], [310], or [3$\bar{1}$0].

were performed using MacTempas software (Kilaas, 1991).

RESULTS

Selected area diffraction (SAD) patterns from several annite grains indicated that they commonly adopt $1M$ and $2M_1$ sequences. More complex diffraction patterns were observed, indicating inhomogeneous polytypes. Occasionally band-like contrast parallel to (001) occurs in both $1M$ and $2M_1$ crystals if observed close to, but slightly away from the [010], [310], or [3$\bar{1}$0] direction (Figure 1). Figure 2a is a lattice image of a similar region to that in Figure 1. The beam direction is slightly away from the [010] direction. Several fringes have more contrast than others, but the periodicity does not vary (~1.0 nm). Note the lack of streaking of 00l reciprocal rows in the SAD patterns (Figure 2b and 2c) which show 1.0-nm spacing. The distinctive contrast in Figures 1 and 2a did not occur if the crystals were observed exactly along the zone axes (*i.e.*, [100] or [010]). Iijima and Buseck (1978) reported that stacking disorder in micas is clearly observed if the crystal is slightly away from the zone axes. Thus, the contrast in Figures 1 and 2a is probably related to stacking irregularity in the crystals. Figure 2b and 2c shows SAD patterns along [$\bar{1}$10] and [010], respectively, from the area in Figure 2a, using a selected-area aperture size corresponding to ~100 nm. The pattern along [$\bar{1}$10] is similar to a $2M_1$ polytype (Figure 2b) except for weak streaks along 11l and 22l reciprocal-lattice rows. These streaks suggest slight disorder; 33l family reflections are not streaked. The pattern along the [010] direction in Figure 2c shows that the 20l row is strongly streaked. This streaking

indicates that reflections with $h \neq 0$ (mod 3) and $k = 0$ (mod 3) are non-family reflections. Therefore, the sequence corresponds to a mixed-rotation polytype, *i.e.*, it contains both (0°, ±120°) and (±60°, 180°) rotations.

Figure 3 shows processed atomic-resolution images from Figure 2a (note the square bracket in Figure 2a) recorded along [$\bar{1}$10] (Figure 3a) and [010] (Figure 3b). The corresponding layers in the two images were identified by counting layers from the chlorite-unit layer at the bottom of the image in Figure 2a, as indicated by the arrow. The corresponding simulated atomic-resolution images are shown in Figure 4. Although minor differences in contrast exist between Figure 3 and Figure 4, this is probably produced by slight crystal misorientation and weak astigmatism. Nevertheless, correspondence between the crystal structure and the contrast of the image in Figure 3 can be made. Black spots corresponding to a pair of (Si, Al)O_4 tetrahedra (along [$\bar{1}$10]) and a single tetrahedron (along [010]) can be identified in Figure 3. The stagger of each tetrahedral sheet with an angle of 0°, 60°, 120°, 180°, -120°, and -60° relative to the b axis observed along the [$\bar{1}$10] direction indicates lateral shifts of 0, $+b/6$, $+b/6$, 0, $-b/6$, and $-b/6$, respectively. On the other hand, these staggers indicate lateral shifts of $+a/6$, $+a/3$ (= $-a/6$), $+a/6$, $-a/6$, $-a/3$ (= $+a/6$), and $-a/6$ if they are observed along [010]. By these two shifts within the same layer (white arrows in Figure 3), the stagger direction of the tetrahedral sheets in each 2:1 layer and, consequently, the stacking sequence can be completely determined. Figure 5 shows the stagger directions of nearly all layers from the bottom to the top in Figure 2a, determined by the analysis of several atomic-resolution images. The bold arrows correspond to the 2:1 layers showing the strong contrast in the lattice image in Figure 2a. On both sides of these layers, stacking sequences with ±60° or 180° rotations are present. Figure 5 also shows that the $2M_1$ sequence (±120° rotations) is dominant, although a few faults occur within the sequence corresponding to the $1M$ stacking mode (0° rotations). The present stacking sequence is reminiscent of that found by Ohta *et al.* (1979) in clintonite (the original name "valuevite" is now considered a variety name of clintonite, according to the IMA report on mica nomenclature: Rieder *et al.*, 1998). In contrast to clintonite, however, the 180° rotations occur extensively, and the overall sequence is a random mixture of $2M_1$ and $2O$. Locally, a $2O$ sequence with six unit layers and a $4A_8$ sequence, corresponding to RTW (Ross-Takeda-Wones) rotational symbols 2233 (Ross *et al.*, 1966; Takeda and Ross 1995), with three unit layers, are formed.

The chemical composition was analyzed with a beam diameter of ~10 nm to examine the compositional change between the area shown in Figure 2a and adjacent areas with the $2M_1$ structure. The results in-
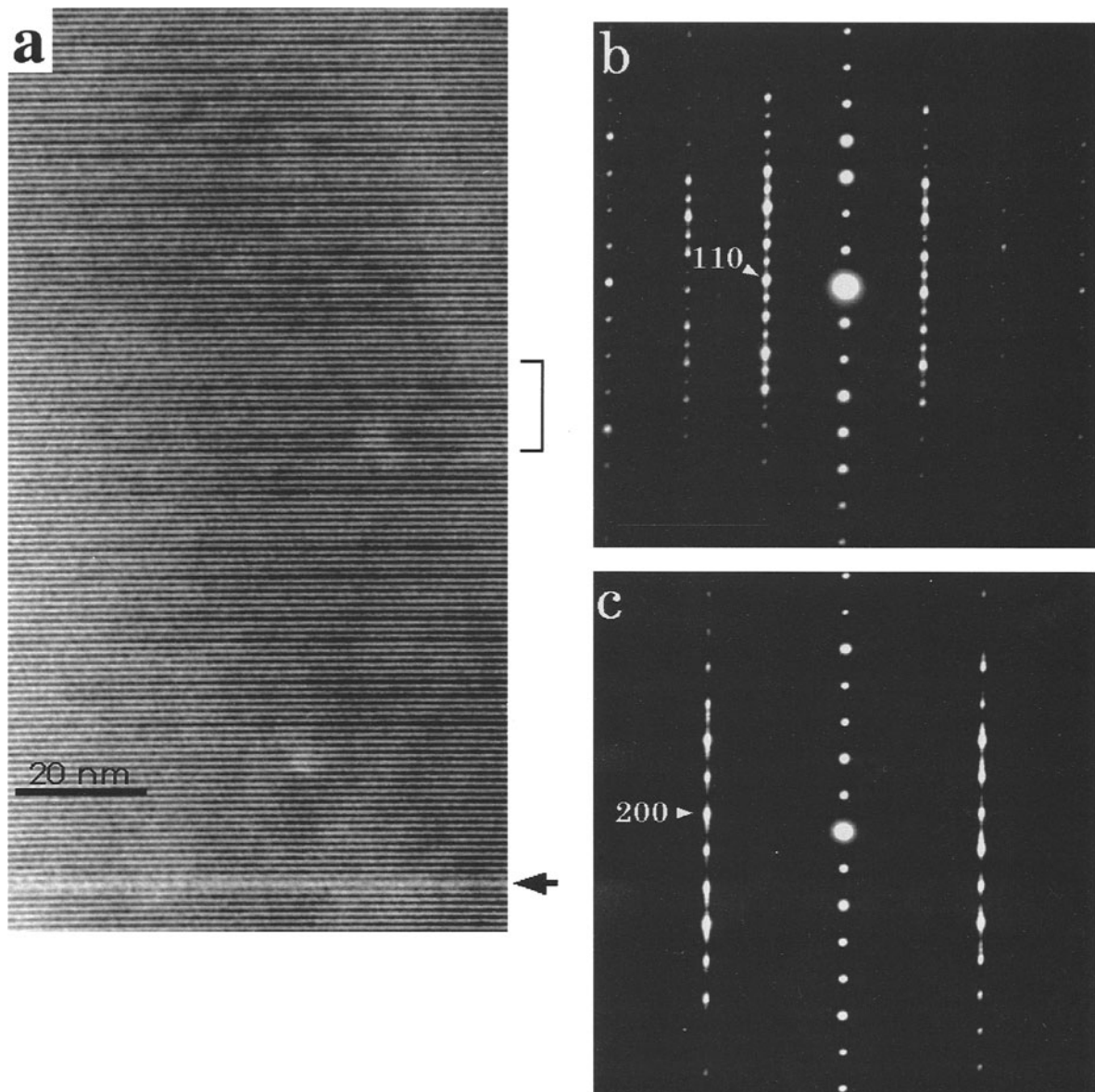
Figure 2. (a) (001) lattice image showing band-like contrast as in Figure 1. The arrow indicates the interlayer transformed to a brucite-like sheet by chloritization. The square bracket is the corresponding area to images in Figure 3. SAD patterns including layers in (a) along [$\bar{1}$10] and [010] are shown in (b) and (c), respectively. Note the strong streak along the 20l row in (c).

dicated no difference within the range of experimental error.

DISCUSSION

As far as we know, this is the second report of a $1M_r$-$n(60°)$ in phyllosilicates and the first for biotite, or the phlogopite-annite series. In contrast with the rotationally disordered illite-smectite reported by McCarty and Reynolds (1995), the annite crystal consists of an ordered $2M_1$ polytype, within which a small disordered region occurs. The analysis and the interpretation differ in the two cases. Clearly, the volume

showing such a sequence is so small that it cannot be detected by conventional diffraction techniques other than small-area electron diffraction. Thus, this reported occurrence may be unique or such (±60°, 180°) rotations may have been overlooked by previous workers who have not considered TEM images of micas along [310], [010], or [$\bar{3}$10], $i.e.$, the orientation for detecting (±60°, 180°) rotations.

From the stacking vectors in Figure 5, the dominant stacking sequence appears to be the $2M_1$ polytype (±120° alternate rotations) for this sample. This sequence is probably perturbed by some event, such as
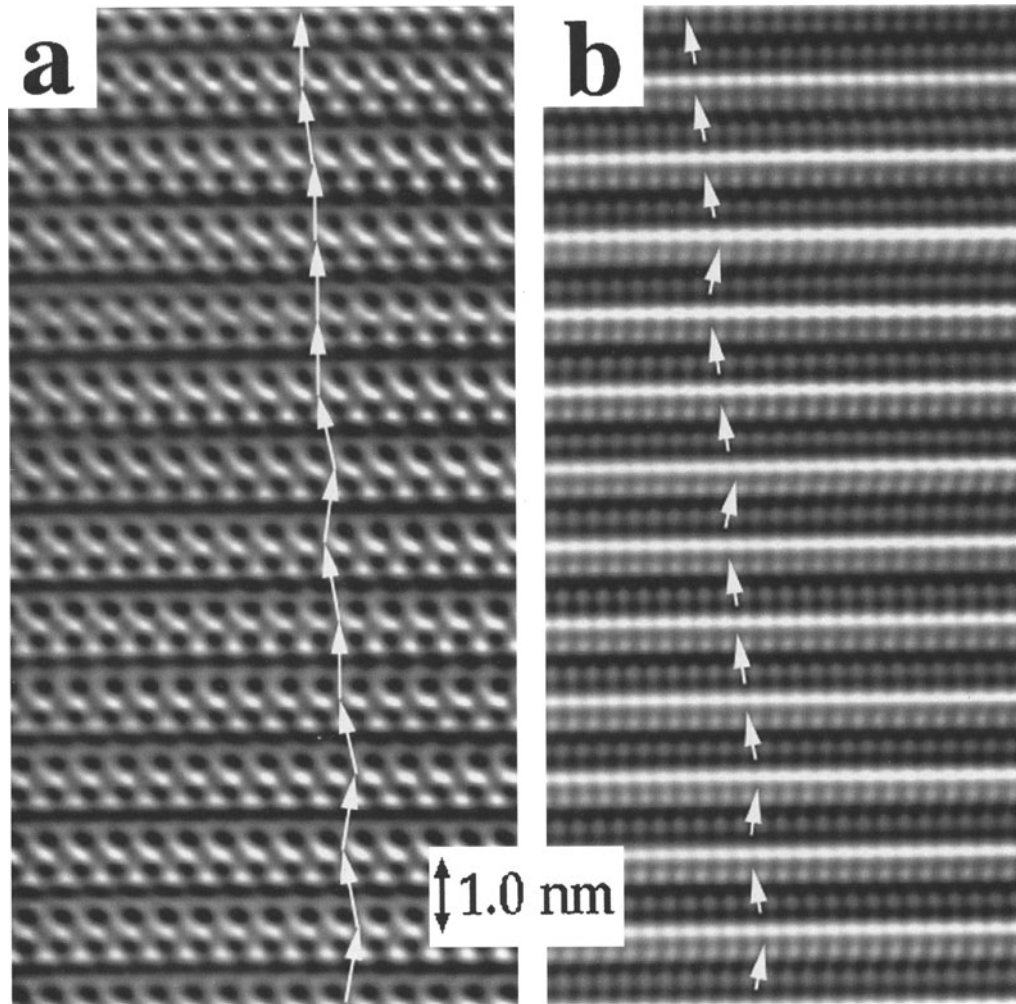
Figure 3.   Filtered atomic-resolution images of the annite layers in Figure 2a, recorded along [Ī10] and [010] in (a) and (b), respectively. These 13 layers in the images correspond to layers No. 58–70 in Figure 5. The white arrows indicate the shift of the tetrahedral sheets in each 2:1 layer. In Figure 3a, the arrows connect dark spots which correspond to potassium ions at the interlayers, the lateral shift of which is the same as that of the stagger of two tetrahedral sheets in a 2:1 layer.

the lateral coalescence of two or more small crystallites, which may introduce one or more layers with different orientation (Baronnet, 1973; Penn and Banfield, 1998; Kogure and Nespolo, 1999). New growth layers may developed at the coalescence point where two crystals come into contact (Sunagawa *et al.*, 1975; Tomura *et al.*, 1978). The disordered region probably formed from the structural adjustment at the interface between the two crystals.

To interpret the stacking sequence in Figure 5, the absolute orientation of layers must be considered, as described by Z symbols (Zvyagin *et al.*, 1979; Zhukhlistov *et al.*, 1990). These symbols give the absolute orientations and relative displacements of half-layers with respect to a space-fixed reference (*a, b*). Within the so-called homo-octahedral approximation (origin of the octahedral sheet at the $M1$ site; see Nespolo *et*

al., 1999) the two half-layers within the same layer have the same orientation and one Z symbol is sufficient to describe the orientation of the whole layer (Zhukhlistov *et al.*, 1990). This orientation is illustrated by the six structure-related a_i axes (i = 1–6). The (001) projection of stacking vectors is indicated by the Z symbol i (i = 1, 2, . . . 6) when the a_i axis is parallel to the *a* space-fixed axis (Figure 5). The parity of Z symbols (odd or even) is commonly called *orientation parity* (Zvyagin, 1997).

In Figure 5, the stacking sequence begins with a $2M_1$ pattern, which consists of layers of the same orientation parity, namely Z = 2 and Z = 4. The pattern of the sequence alteration in the first 51 layers is straightforward: one layer with abnormal orientation (Z = 5) replaces one layer of the $2M_1$ sequence in an irregular way. For layers No. 19, 23, 25, and 31, a
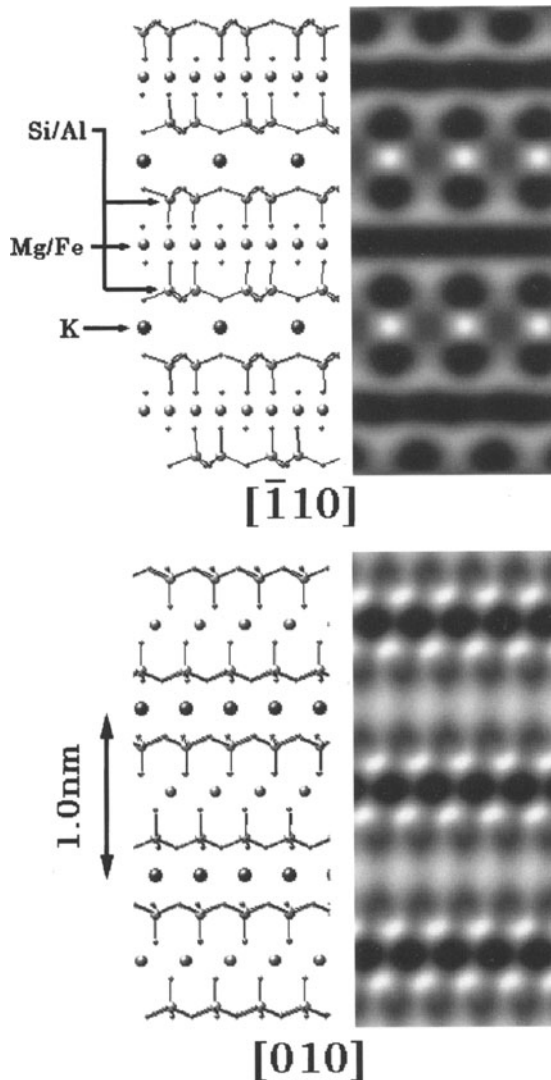
Figure 4.   Crystal structure models of annite and corresponding multi-slice simulated images along [$\bar{1}$10] and [010]. The specimen thickness and defocus value in the simulation are 5 and 40 nm (underfocus), respectively.
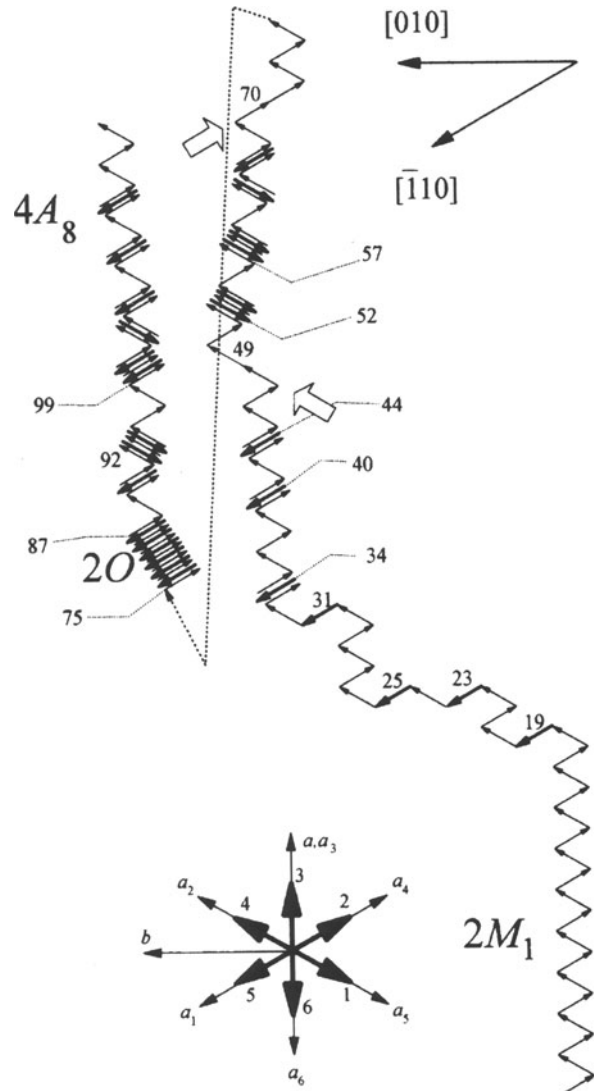

Figure 5.   The stacking sequences of annite layers, from the bottom to the top in Figure 2a. The bold arrows correspond to the 2:1 layers that show strong contrast in Figure 2a. Inset: Z symbols and vectors in projection on the (001) plane with reference to the space-fixed setting (a, b axes). The structure-fixed axes a_1–a_6 are shown also. Along the stacking vectors, sequence numbers are shown in correspondence of layers with orientation different from that of the matrix (see text).

layer with orientation $Z = 5$ occurs instead of a layer with orientation $Z = 2$, as expected for the $2M_1$ sequence. Similarly, for layers No. 34, 40, and 44, a layer with orientation $Z = 5$ occurs instead of a layer with orientation $Z = 4$. In the former case ($Z = 5$ instead of $Z = 2$), 60° rotations are generated relative to adjacent "normal" layers with $Z = 4$, and in the latter case ($Z = 5$ instead of $Z = 4$), 180° rotations are generated. The layer with $Z = 5$ may have originated by the protrusion of a foreign crystallite, which then altered the spiral growth of the $2M_1$ crystal.

From layer No. 52, layers with $Z = 1$ and longer $2O$-like sequences with more than three layers occur. Note that these sequences occur only after the occurrence of a $1M$-like sequence (layers No. 48–49, indi-

cated by the white arrow near No. 44). In a $2M_1$ sequence, layer No. 49 should be $Z = 2$, but this layer has orientation $Z = 4$, rotated counterclockwise by 120° relative to $Z = 2$. Layer No. 52 has orientation $Z = 1$ (120° counterclockwise rotation from $Z = 5$, the original orientation of the "abnormal" layer). Thus a structural adjustment at layer No. 49 has probably influenced the orientation both of the matrix and of the abnormal layer. The five-layer (No. 51–55; 57–61; 92–96; 99–103) and 13-layer (No. 75–87) $2O$-like sequences cannot be interpreted as the three-layer se-

quences described above. A series of structural adjustments appears to be active from layer No. 49 to the end of the disorder sequence (the 13-layer $2O$-like sequence occurs again after a $1M$-like sequence; No. 70–71, indicated by the white arrow near No. 70), to produce thereafter the $2M_1$ polytype.

The modifying event may have been the lateral coalescence of crystallites. The chemistry of the sample, however, may have been important also for the true $2O$-like sequences. The composition of the sample is not unusual, but it contains a significant amount of Fe and Ti, two elements which are commonly associated with inhomogeneous polytypes. High Fe content in octahedral sites is preferable to ($\pm 60°$, $180°$) rotational sequences because it increases the lateral dimension of the octahedral sheet and decreases ditrigonal rotation, thereby allowing lateral congruence between the two sheets (Takeda and Mori, 1970; Hazen and Wones, 1972; McCarty and Reynolds, 1995). This is especially true at high temperature (Takeda and Morosin, 1975; Russell and Guggenheim, 1999). Therefore, the interlayer coordination polyhedron does not differ greatly between subfamilies A and B.

The effect of Ti on the structure of the 2:1 layer is not known. A high Ti/(Ti + Fe$_{tot}$) ratio favors $\pm 120°$ stacking angles over angles of $0°$ (Baronnet *et al.*, 1993). The addition of Ti during the synthesis of micas influences growth kinetics and modifies the growth habit (Sun and Baronnet, 1989). The presence of the high-charge Ti in the octahedral sheet must affect the position and species of neighboring cations, especially those in the tetrahedral sites. These adjustments are local and differ from the observed average structure obtained by X-ray analyses. The effect of Ti on the local structure of mica requires further investigation. However, the association of Ti with inhomogeneous polytypes and rare sequences with stacking errors can hardly be considered casual.

ACKNOWLEDGMENTS

REFERENCES

Amouric, M. and Baronnet, A. (1983) Effect of early nucleation conditions on synthetic muscovite polytypism as seen by high resolution transmission electron microcopy. *Physics and Chemistry of Minerals*, **9**, 146–159.

Backhaus, K.-O. and Ďurovič, S. (1984) Polytypism of micas. I. MDO polytypes and their derivation. *Clays and Clay Minerals*, **32**, 453–463.

Bailey, S.W. (1980) Crystal Chemistry of True Micas. In *Micas, Reviews in Mineralogy, Volume 13*, S.W. Bailey, ed., Mineralogical Society of America, Washington D.C., 13–60.

Bailey, S.W. (1988) X-ray diffraction identification of the polytypes of mica, serpentine, and chlorite. *Clays and Clay Minerals*, **36**, 193–213.

Banfield, J.F. and Murakami, T. (1998) Atomic-resolution transmission electron microscope evidence for the mechanism by which chlorite weathers to 1:1 semi-regular chlorite-vermiculite. *American Mineralogist*, **83**, 348–357.

Baronnet, A. (1973) Sur les origines des dislocations vis et des spirales de croissance dans les micas. *Journal of Crystal Growth*, **19**, 193–198.

Baronnet, A. (1980) Polytypism in micas: A survey with emphasis on the crystal growth aspects. In *Current Topics in Materials Science, Volume 5*, E. Kaldis, ed., North-Holland Publishing Company, Amsterdam, 447–548.

Baronnet, A. and Amouric, M. (1986) Growth spirals and complex polytypism in micas. II. Occurrence frequencies in synthetic species. *Bulletin de Minéralogie*, **109**, 489–508.

Baronnet, A. and Kang, Z.C. (1989) About the origin of mica polytypes. *Phase Transitions*, **16/17**, 477–493.

Baronnet, A., Nitsche, S., and Kang, Z.C. (1993) Layer stacking microstructures in a biotite single crystal. A combined HREM-AEM study. *Phase Transitions*, **43**, 107–128.

Belov, N.V. (1949) The twin laws of micas and micaceous minerals. *Mineralogicheskii sbornik L'vovskogo geologicheskogo obshchestva (L'vov university)*, **3**, 29–40. (in Russian).

Drits, V.A. and McCarty, D.K. (1996) The nature of diffraction effects from illite and illite/smectite consisting of interstratified *trans*-vacant and *cis*-vacant 2:1 layers; A semiquantitative technique for determination of layer-type content. *American Mineralogist*, **81**, 852–863.

Drits, V.A. and Tchoubar, C. (1990) *X-ray Diffraction by Disordered Lamellar Structures*. Springer Verlag, New York, 371 pp.

Drits, V.A., Zvyagin, B.B., and Tokmakov, P.P. (1966) Gümbelite—A dioctahedral mica $2M_2$. *Transactions (Doklady) Academy Sciences SSSR: Earth Science Section*, **170**, 156–159.

Drits, V.A., Plançon, B.A., Sakharov, B.A., Besson, G., Tsipursky, S.I., and Tchoubar, C. (1984) Diffraction effect calculated for structural models of K-saturated montmorillonite containing different types of defects. *Clay Minerals*, **19**, 541–561.

Ďurovič, S. and Weiss, Z. (1986) OD structures and polytypes. *Bulletin de Minéralogie*, **109**, 15–29.

Ďurovič, S., Weiss, Z., and Backhaus, K.-O. (1984) Polytypism of micas. II. Classification and abundance of MDO polytypes. *Clays and Clay Minerals*, **32**, 454–474.

Ferrow, E.A. and Roots, M. (1989) A preparation technique for TEM specimens; application to synthetic Mg-chlorite. *European Journal of Mineralogy*, **1**, 815–819.

Filut, M.A., Rule, A.C., and Bailey, S.W. (1985) Crystal structure refinement of anandite-$2Or$, a barium- and sulfur-

bearing trioctahedral mica. *American Mineralogist,* **70,** 1298–1308.

Giuseppetti, G. and Tadini, C. (1972) The crystal structure of 2*O* brittle mica: anandite. *Tschermaks Mineralogische und Petrographische Mitteilungen,* **18,** 169–184.

Hazen, R.M. and Wones, D.R. (1972) The effect of cation substitutions on the physical properties of trioctahedral micas. *American Mineralogist,* **57,** 103–129.

Iijima, S. and Buseck, P.R. (1978) Experimental study of disordered mica structure by high-resolution electron microscopy. *Acta Crystallographica,* **A34,** 709–719.

Kilaas, R. (1991) HREM image simulation. In *Proceeding of 49th Electron Microscope Society of America Meeting, San Francisco,* G.W. Bailey, ed., San Francisco Press, San Francisco, 528–529.

Kogure, T. and Banfield, J.F. (1998) Direct identification of the six polytypes of chlorite characterized by semi-random stacking. *American Mineralogist,* **83,** 925–930.

Kogure, T. and Murakami, T. (1996) Direct identification of biotite/vermiculite layers in hydrobiotite using high-resolution TEM. *Mineralogical Journal,* **18,** 131–137.

Kogure, T. and Nespolo, M. (1999) A TEM study of long-period mica polytypes: Determination of the stacking sequence of oxybiotite by means of atomic-resolution images and periodic intensity distribution (PID). *Acta Crystallographica,* **B55,** 507–516.

Mauguin, M.Ch. (1928) Etude de Micas au moyen du rayons X. *Bulletin de la Societé Française de Minéralogie et Cristallografie,* **51,** 285–332.

McCarty, D.K. and Reynolds, R.C., Jr. (1995) Rotationally disordered illite/smectite in Paleozoic K-bentonites. *Clays and Clay Minerals,* **43,** 271–284.

Nespolo, M. (1999) Analysis of family reflections of OD mica polytypes, and its application to twin identification. *Mineralogical Journal,* **21,** 53–85.

Nespolo, M. and Takeda, H. (1999) Inhomogeneous mica polytypes: 8-layer polytype of the 2*M*₁ structural series determined by the periodic intensity distribution (PID) analysis of the X-ray diffraction pattern. *Mineralogical Journal,* **21,** 103–118.

Nespolo, M., Takeda, H., and Ferraris, G. (1997) Crystallography of mica polytypes. In *Modular Aspects of Minerals/ EMU Notes in Mineralogy, Volume 1,* S. Merlino, ed., Eötvös University Press, Budapest, 81–118.

Nespolo, M., Takeda, H., and Ferraris, G. (1998) Representation of the axial settings of mica polytypes. *Acta Crystallographica,* **A54,** 348–356.

Nespolo, M., Takeda, H., Kogure, T., and Ferraris, G. (1999) periodic intensity distribution (PID) of mica polytypes: Symbols, structural model orientation and axial settings. *Acta Crystallographica,* **A55,** 659–676.

Ni, Y. and Hughes, J.M. (1996) The crystal structure of nanpingite-2*M*₂, the Cs end-member of muscovite. *American Mineralogist,* **81,** 105–110.

Ochi, S. (1982) The Ryoke granitic rocks in the Takanawa Peninsula, Shikoku, Japan. *Journal of the Geological Society of Japan,* **88,** 511–512. (in Japanese).

Ohta, T., Takéuchi, Y., and Takeda, H. (1979) Structural study of brittle micas (II). Statistical mode of stacking sequence in a valuevite crystal as deduced by computer simulation. *Mineralogical Journal,* **9,** 1–15.

Penn, R.L. and Banfield, J.F. (1998) Imperfect oriented attachment: Dislocation generation in defect-free nanocrystals. *Science,* **281,** 969–971.

Radoslovich, E.W. (1959) Structural control of polymorphism in micas. *Nature,* **163,** 253.

Ramsdell, L.S. (1947) Studies on silicon carbide. *American Mineralogist,* **32,** 64–82.

Reynolds, R.C. (1993) Three-dimensional powder X-ray diffraction from disordered illite: Simulation and interpretation of the diffraction patters. In *CMS Workshop Lectures, Volume 5: Computer Applications to X-ray Powder Diffraction Analysis of Clay Minerals,* R.C. Reynolds, Jr. and J.R. Walkers, eds., The Clay Minerals Society, Boulder, Colorado, 43–77.

Rieder, M., Huka, M., Kučerová, D., Minařík, L., Obermajer, J., and Povondra, P. (1970) Chemical composition and physical properties of lithium-iron micas from the Krušné hory Mts. (Erzgebirge). *Contributions to Mineralogy and Petrology,* **27,** 131–158.

Rieder, M., Cavazzini, G., D'yakonov, Yu, S., Frank-Kamenetskii, V.A., Gottardi, G., Guggenheim, S., Koval', P.V., Müller, G., Neiva, A.M.R., Radoslowich, E.W., Robert, J.L., Sassi, F.P., Takeda, H., Weiss, Z., and Wones, D.R. (1998) Nomenclature of the micas. *Canadian Mineralogist,* **36,** 905–912.

Ross, M., Takeda, H., and Wones, D.R. (1966) Mica polytypes: Systematic description and identification. *Science,* **151,** 191–193.

Russell, R.L. and Guggenheim, S. (1999) Crystal structure of near-end-member phlogopite at high temperatures and heat-treated Fe-rich phlogopite: The influence of the O, OH, F site. *Canadian Mineralogist,* **37,** 711–720.

Smith, J.V. and Yoder, H.S. (1956) Experimental and theoretical studies of the mica polymorphs. *Mineralogical Magazine,* **31,** 209–235.

Sun, B.N. and Baronnet, A. (1989) Hydrothermal growth of OH-phlogopite single crystals II. Role of Cr and Ti adsorption on crystal growth rates. *Chemical Geology,* **78,** 301–314.

Sunagawa, I., Koshino, Y., Asakura, M., and Yamamoto, T. (1975) Growth mechanism of some clay minerals. *Fortschritte der Mineralogie,* **52,** 217–224.

Takeda, H. (1967) Determination of the layer stacking sequence of a new complex mica polytype: A 4-layer lithium fluorophlogophite. *Acta Crystallographica,* **22,** 845–853.

Takeda, H. and Burnham, C.W. (1969) Fluor-polylithionite: A lithium mica with nearly hexagonal $Si_2O_5^{2-}$ ring. *Mineralogical Journal,* **6,** 102–109.

Takeda, H. and Mori, N. (1970) Crystal chemistry of rock-forming silicate minerals. II. Exsolutions and structural variations of solid solutions. *Journal of the Crystallographic Society of Japan,* **12,** 231–248. (in Japanese).

Takeda, H. and Morosin, B. (1975) Comparison of observed and predicted parameters of mica at high temperature. *Acta Crystallographica,* **B31,** 2444–2452.

Takeda, H. and Ross, M. (1995) Mica polytypism: Identification and origin. *American Mineralogist,* **80,** 715–724.

Takeda, H., Haga, N., and Sadanaga, R. (1971) Structural investigation of polymorphic transition between 2*M*₂-, 1*M*-lepidolite and 2*M*₁-muscovite. *Mineralogical Journal,* **6,** 203–215.

Takéuchi, Y. and Sadanaga, R. (1959) The crystal structure of xanthophyllite. *Acta Crystallographica,* **12,** 945–946.

Tomura, S., Kitamura, M., and Sunagawa, I. (1978) High resolution electron microscopy of dioctahedral mica. *Mineralogical Journal,* **9,** 129–136.

Weiss, Z. and Wiewióra, A. (1986) Polytypism of micas. III. X-ray diffraction identification. *Clays and Clay Minerals,* **34,** 53–68.

Zhukhlistov, A.P., Zvyagin, B.B., Soboleva, S.V., and Fedotov, A.F. (1973) The crystal structure of the dioctahedral mica 2*M*₂ determined by high voltage electron diffraction. *Clays and Clay Minerals,* **21,** 465–470.

Zhukhlistov, A.P., Zvyagin, B.B., and Pavlishin, V.I. (1990) Polytypic 4M modification of Ti-biotite with nonuniform alternation of layers, and its appearance in electron-diffrac-

tion patterns from textures. *Soviet Physics Crystallography,* **35,** 232–236.

Zvyagin, B.B. (1967) *Electron Diffraction Analysis of Clay Mineral Structures.* Plenum Press, New York, 364 pp.

Zvyagin, B.B. (1988) Polytypism of crystal structures. *Computer Mathematics Applications,* **16,** 569–591.

Zvyagin, B.B. (1997) Modular analysis of crystal structures. In *Modular Aspects of Minerals/EMU Notes in Mineralogy, Volume 1,* S. Merlino, ed., Eötvös University Press, Budapest, 345–372.

Zvyagin, B.B., Vrublevskaya, Z.V., Zhukhlistov, A.P., Sidorenko, O.V., Soboleva, S.V., and Fedotov, A.F. (1979) *High-Voltage Electron Diffraction in the Study of Layered Minerals.* Nauka Press, Moscow, 224 pp. (in Russian).